



UNIVERSITY OF LEEDS

This is a repository copy of *Towards a time-domain modeling framework for small-signal analysis of unbalanced microgrids*.

White Rose Research Online URL for this paper:
<http://eprints.whiterose.ac.uk/114880/>

Version: Accepted Version

Proceedings Paper:

Ojo, Y and Schiffer, JF orcid.org/0000-0001-5639-4326 (2017) Towards a time-domain modeling framework for small-signal analysis of unbalanced microgrids. In: 2017 IEEE Manchester PowerTech. 12th IEEE PES PowerTech Conference, 18-22 Jun 2017, Manchester, UK. IEEE . ISBN 978-1-5090-4237-1

<https://doi.org/10.1109/PTC.2017.7981013>

© 2017 IEEE. Personal use of this material is permitted. Permission from IEEE must be obtained for all other uses, in any current or future media, including reprinting/republishing this material for advertising or promotional purposes, creating new collective works, for resale or redistribution to servers or lists, or reuse of any copyrighted component of this work in other works.

Reuse

Unless indicated otherwise, fulltext items are protected by copyright with all rights reserved. The copyright exception in section 29 of the Copyright, Designs and Patents Act 1988 allows the making of a single copy solely for the purpose of non-commercial research or private study within the limits of fair dealing. The publisher or other rights-holder may allow further reproduction and re-use of this version - refer to the White Rose Research Online record for this item. Where records identify the publisher as the copyright holder, users can verify any specific terms of use on the publisher's website.

Takedown

If you consider content in White Rose Research Online to be in breach of UK law, please notify us by emailing eprints@whiterose.ac.uk including the URL of the record and the reason for the withdrawal request.



eprints@whiterose.ac.uk
<https://eprints.whiterose.ac.uk/>

Towards a time-domain modeling framework for small-signal analysis of unbalanced microgrids

Yemi Ojo and Johannes Schiffer
School of Electronic and Electrical Engineering
University of Leeds
Leeds, UK

Abstract—Small-signal analysis is one of the most frequently used techniques to assess the operating conditions of power systems. Typically, this analysis is conducted by employing a phasor-based model of the power network derived under the assumption of balanced operating conditions. However, distribution networks and, amongst these, microgrids are often unbalanced. Hence, their analysis requires the development of tools and methods valid under such conditions. Motivated by this, we propose a modeling approach for generic nonlinear and unbalanced three-phase microgrids, which allows to derive a small-signal model in a standard fashion. The approach is based on a time-domain decomposition of the electrical waveforms in positive and negative synchronous reference frames. The efficacy of the approach is demonstrated via application to an exemplary unbalanced microgrid.

Index Terms—Microgrids; unbalanced power systems; small-signal analysis; time-domain modeling of power systems

I. INTRODUCTION

The conventional power system is centred around generators that depend mostly on conventional fuel to produce electricity. Since fossil-fueled power generation substantially contributes to greenhouse gas emissions, increasing efforts towards the exploration of renewable energy sources (RES) are being made. For example, the EU governments aim at achieving an emission reduction of at least 80% by 2050 [1]. As most of these renewable sources are small-scale distributed generation (DG) units, they are often connected at the low and medium voltage levels, rather than directly to the transmission system. Hence, there is an increasing amount of generation capacity present in the distribution network [2]. The efficient and reliable integration of these units requires the development of new operation concepts, amongst which the microgrid has been identified as one of the most promising [1]–[4].

A microgrid is a subset of a larger distribution network and is formed by several DG units, loads and storage elements [2]–[4]. A key feature of a microgrid is that it can operate connected to the main grid, but also in a completely isolated manner, hence increasing the resiliency of the overall power system [1]. Compared to conventional power systems, a predominant feature of microgrids is that most of their generation is inverter-interfaced [4]. This fact leads to different network

dynamics and poses many technical challenges to ensure a reliable network operation.

System stability has been identified as one of the most relevant and critical objectives for microgrid operation [5], [6]. Thus far, most work on stability of microgrids is conducted under the assumption of balanced operating conditions [7]–[11]. Yet, microgrids are often unbalanced due to various factors, including uneven distribution of load or generation across the three-phases as well as single-phase laterals [4], [6], [12]. Arguably, the presence of unbalances can significantly deteriorate the system performance and even lead to instability [13]–[16]. Hence, in order to fully grasp the characteristics of the system it is important to explicitly consider these phenomena when analyzing its stability properties [13]–[16].

In that regard, by invoking an assumption on the net torque of the generator a phasor-based model of an unbalanced power system has been derived in [14], [15] and used to assess the small-signal stability of a synchronous generator (SG) based unbalanced power system. A related analysis has been conducted in [13] via a modal estimation approach using the Prony method. Furthermore, a simulation algorithm to assess stability of an unbalanced microgrid has been proposed in [6].

Another possibility for modeling unbalanced power systems are dynamic phasors [17]–[19]. The dynamic phasor concept uses generalized averaging to approximate a given waveform by a finite sum of the complex coefficients of its Fourier series. Dynamic phasors have recently been used in [16] for modeling and small-signal analysis of an unbalanced radial distribution system. However, as outlined in [13]–[16], there is no standard method for stability assessment of unbalanced power systems available.

Motivated by the above discussion, the present paper provides a time-domain modeling framework for microgrids that is suitable for a small-signal analysis under unbalanced operating conditions. As a small-signal analysis is based on the linearization of the system dynamics, it is convenient to at first perform a coordinate transformation that maps periodic three-phase waveforms to constant DC quantities. Under *balanced* conditions, this can be easily achieved by employing the standard $dq0$ -transformation, see [20], [21]. However, under *unbalanced* conditions the standard $dq0$ -transformation does not yield the desired result. The same applies to the multiple reference frame approach presented in [22]. To overcome

The project leading to this manuscript has received funding from the European Union's Horizon 2020 research and innovation programme under the Marie Skłodowska-Curie grant agreement No. 734832.

this problem and inspired by [23]–[25], we employ a 3-step coordinate transformation based on the "signal delay cancellation" approach to represent the electrical waveforms in their respective positive and negative synchronous reference frames. To the best of our knowledge, this transformation has thus far only been used for control design under unbalanced conditions, see [23]–[25], but not—as in the present case—for the derivation of microgrid models suitable for small-signal analysis. We remark that, in addition to microgrids, the approach can equivalently be applied to other types of unbalanced nonlinear power networks on both the distribution and the transmission level. The proposed modeling framework is validated in simulation and a small-signal model of an exemplary unbalanced microgrid is derived.

II. A TIME-DOMAIN MODELING APPROACH FOR STABILITY ANALYSIS OF UNBALANCED MICROGRIDS

We consider a generic microgrid model represented by the system of coupled differential equations

$$\boxed{\begin{aligned} \dot{x}_{abc}(t) &= f(x_{abc}(t), y_z(t)), & y_x(t) &= h(x_{abc}(t)), \\ \dot{z}(t) &= g(z(t), y_x(t)), & y_z(t) &= w(z(t)), \end{aligned}} \quad (1)$$

where the state vector $x_{abc}(t) \in \mathbb{R}^{3n}$ represents, possibly unbalanced, three-phase waveforms of the electrical part of the system at time $t \geq 0$ and the vector $z(t) \in \mathbb{R}^m$ represents other non-three-phase states, e.g., controller states, communication signals or power measurements as employed in standard generator or converter controls [5], [26]. The output of the electrical system is denoted by $y_x(t) \in \mathbb{R}^l$, while that of the z -dynamics is denoted by $y_z(t) \in \mathbb{R}^q$.

A. Employed coordinate transformation

The employed coordinate transformation is conducted under the following assumption, a physical discussion of which is given in Remark 1 below.

Assumption 1: The system (1) possesses a synchronized solution¹ $(x^*(t), z^*(t)) \in \mathbb{R}^{(3n+m)}$, where $z^*(t) = z^*$ is constant and all three-phase electrical variables $x_{abc}^*(t)$ possess constant amplitude and evolve with a constant frequency $\omega^* \in \mathbb{R}$.

To present the coordinate transformation, we define the constant $T_{f^*} = 1/f^*$, where $f^* = \omega^*/(2\pi)$. Consider the synchronized unbalanced three-phase waveform $x_{abc,i}$ at the i -th node of the microgrid at time t , i.e., $x_{abc,i}(t)$ and the same waveform delayed by $\tau = T_{f^*}/4$, i.e., $x_{abc,i}(t - \tau)$. Furthermore, let

$$\theta^+(t) = \omega^*t, \quad \theta^-(t) = -\omega^*t \quad (2)$$

¹For vectors $x_1 \in \mathbb{R}^n$ and $x_2 \in \mathbb{R}^m$, the notation $x = (x_1, x_2)$ denotes the column vector $x = [x_1^\top \quad x_2^\top]^\top \in \mathbb{R}^{n+m}$.

and recall the $\alpha\beta\gamma$ - and $dq0$ -transformation matrices

$$T_{\alpha\beta\gamma} = \sqrt{\frac{2}{3}} \begin{bmatrix} 1 & -\frac{1}{2} & -\frac{1}{2} \\ 0 & \frac{\sqrt{3}}{2} & -\frac{\sqrt{3}}{2} \\ \frac{1}{\sqrt{2}} & \frac{1}{\sqrt{2}} & \frac{1}{\sqrt{2}} \end{bmatrix}, \quad (3)$$

$$T_{dq0}(\cdot) = \begin{bmatrix} \cos(\cdot) & \sin(\cdot) & 0 \\ -\sin(\cdot) & \cos(\cdot) & 0 \\ 0 & 0 & 1 \end{bmatrix}.$$

Inspired by [23]–[25], consider the transformation matrix

$$\boxed{T(t) = \tilde{T}_{dq0}(t)T_{(+ - 0)}\tilde{T}_{\alpha\beta\gamma},} \quad (4)$$

where

$$\tilde{T}_{dq0}(t) = \begin{bmatrix} T_{dq0}(\theta^+(t)) & \mathbf{0}_{3 \times 3} \\ \mathbf{0}_{3 \times 3} & T_{dq0}(\theta^-(t)) \end{bmatrix}, \quad (5)$$

$$T_{(+ - 0)} = \frac{1}{2} \begin{bmatrix} 1 & 0 & 0 & 0 & -1 & 0 \\ 0 & 1 & 0 & 1 & 0 & 0 \\ 0 & 0 & 1 & 0 & 0 & 0 \\ 1 & 0 & 0 & 0 & 1 & 0 \\ 0 & 1 & 0 & -1 & 0 & 0 \\ 0 & 0 & 0 & 0 & 0 & 1 \end{bmatrix}, \quad (6)$$

as well as

$$\tilde{T}_{\alpha\beta\gamma} = \begin{bmatrix} T_{\alpha\beta\gamma} & \mathbf{0}_{3 \times 3} \\ \mathbf{0}_{3 \times 3} & T_{\alpha\beta\gamma} \end{bmatrix}. \quad (7)$$

Note that $T_{(+ - 0)}$ has full rank and $\tilde{T}_{dq0}(t)$ as well as $\tilde{T}_{\alpha\beta\gamma}$ are unitary matrices. Thus,

$$T^{-1}(t) = \tilde{T}_{\alpha\beta\gamma}^\top T_{(+ - 0)}^{-1} \tilde{T}_{dq0}^\top(t). \quad (8)$$

Then, our employed coordinate transformation is given by

$$\boxed{x_{dq0,i}^{+-}(t) = \begin{bmatrix} x_{dq0,i}^+(t) \\ x_{dq0,i}^-(t) \end{bmatrix} = T(t) \begin{bmatrix} x_{abc,i}(t) \\ x_{abc,i}(t - \tau) \end{bmatrix},} \quad (9)$$

where the vectors

$$x_{dq0,i}^+(t) = \begin{bmatrix} x_{d,i}^+(t) \\ x_{q,i}^+(t) \\ x_{0,i}^+(t) \end{bmatrix}, \quad x_{dq0,i}^-(t) = \begin{bmatrix} x_{d,i}^-(t) \\ x_{q,i}^-(t) \\ x_{0,i}^-(t) \end{bmatrix}$$

denote the positive, negative and zero components at time t in a synchronous reference frame rotating at $+\omega^*$, respectively $-\omega^*$. Furthermore, by writing $T^{-1}(t)$ as

$$T^{-1}(t) = \begin{bmatrix} \mathcal{T}_t(t) \\ \mathcal{T}_\tau(t) \end{bmatrix} \in \mathbb{R}^{6 \times 6}, \quad \mathcal{T}_t \in \mathbb{R}^{3 \times 6}, \quad \mathcal{T}_\tau \in \mathbb{R}^{3 \times 6},$$

we obtain

$$\boxed{\begin{aligned} x_{abc,i}(t) &= \mathcal{T}_t(t)x_{dq0,i}^{+-}(t), \\ x_{abc,i}(t - \tau) &= \mathcal{T}_\tau(t)x_{dq0,i}^{+-}(t). \end{aligned}} \quad (10)$$

As can be seen from (4), the employed transformation matrix $T(t)$ consists of the joint execution of three individual steps. First, the waveforms $x_{abc,i}(t)$ and $x_{abc,i}(t - \tau)$ are transformed into $\alpha\beta\gamma$ -coordinates via the Clarke transformation. Second, in $\alpha\beta\gamma$ -coordinates the positive and negative sequences are extracted via the "signal delay cancellation" approach as

employed in [23]–[25]. The third and final transformation step consists of transforming the obtained positive and negative sequences into $dq0$ coordinates via the standard $dq0$ -transformation. To illustrate the coordinate transformation, consider the exemplary unbalanced three-phase waveform

$$v_{abc}(t) = \begin{bmatrix} v_a(t) \\ v_b(t) \\ v_c(t) \end{bmatrix} = \sqrt{2} \begin{bmatrix} V_a \sin(\omega^* t) \\ V_b \sin(\omega^* t - \frac{2\pi}{3}) \\ V_c \sin(\omega^* t + \frac{2\pi}{3}) \end{bmatrix}.$$

With $\theta^+(t)$, $\theta^-(t)$ given in (2) and $T(t)$ given in (9), we obtain

$$v_{dq0}^{+-}(t) = T(t) \begin{bmatrix} v_{abc}(t) \\ v_{abc}(t - \tau) \end{bmatrix} = \begin{bmatrix} 0 \\ -\frac{2}{\sqrt{3}}(V_a + V_b + V_c) \\ v_0^+ \\ V_b - V_c \\ \frac{1}{\sqrt{3}}(2V_a - V_b - V_c) \\ v_0^- \end{bmatrix},$$

where

$$v_0^+ = \frac{1}{\sqrt{3}}(v_a(t) + v_b(t) + v_c(t)),$$

$$v_0^- = \frac{1}{\sqrt{3}}(v_a(t - \tau) + v_b(t - \tau) + v_c(t - \tau)).$$

Clearly, v_d^+ , v_q^+ , v_d^- , v_q^- are constant, while the zero components are oscillating at the synchronized frequency ω^* . Furthermore, if v_{abc} is balanced, i.e., $V_a = V_b = V_c$, we have that $v_{dq0}^- = \mathbf{0}_3$ and recover the standard $dq0$ -coordinates under balanced conditions, see [20], [25] and [21].

Remark 1: In the presence of unbalances, the three-phase power flows in the network contain components oscillating at $\pm 2\omega$ [13]–[15], [25]. Therefore, when used for control purposes, the measured powers of the individual units are typically passed through a low-pass filter in order to obtain the fundamental component of the powers [5], [7], [21], see also Section III. Then the resulting frequency is approximately constant and, thus, Assumption 1 is valid. An extension of the proposed modeling procedure to scenarios with time-varying synchronous frequency is currently under investigation.

B. Transformation of generic microgrid model

We apply the coordinate transformation (9) to the model (1). To this end, we recall that the mapping $T(t)$ in (4) is time-dependent. Straightforward calculations yield

$$\begin{aligned} \dot{x}_{dq0,i}^{+-}(t) &= T(t) \begin{bmatrix} \dot{x}_{abc,i}(t) \\ \dot{x}_{abc,i}(t - \tau) \end{bmatrix} + \frac{dT(t)}{dt} \begin{bmatrix} x_{abc,i}(t) \\ x_{abc,i}(t - \tau) \end{bmatrix} \\ &= T(t) \begin{bmatrix} \dot{x}_{abc,i}(t) \\ \dot{x}_{abc,i}(t - \tau) \end{bmatrix} + \frac{dT(t)}{dt} T^{-1}(t) x_{dq0,i}^{+-}(t) \\ &= T(t) \begin{bmatrix} \dot{x}_{abc,i}(t) \\ \dot{x}_{abc,i}(t - \tau) \end{bmatrix} + \mathcal{P} x_{dq0,i}^{+-}(t), \end{aligned}$$

where we defined the constant matrix

$$\mathcal{P} := \frac{dT(t)}{dt} T^{-1}(t) = \omega^* \begin{bmatrix} \tilde{T} & \mathbf{0}_{3 \times 3} \\ \mathbf{0}_{3 \times 3} & \tilde{T}^\top \end{bmatrix}, \quad \tilde{T} = \begin{bmatrix} 0 & 1 & 0 \\ -1 & 0 & 0 \\ 0 & 0 & 0 \end{bmatrix}. \quad (11)$$

By introducing the short-hands

$$\begin{aligned} \bar{x}_{abc,i}(t, \tau) &= (x_{abc,i}(t), x_{abc,i}(t - \tau)), \\ \bar{x}_{abc}(t, \tau) &= (\bar{x}_{abc,1}(t, \tau), \dots, \bar{x}_{abc,n}(t, \tau)), \end{aligned} \quad (12)$$

and using the Kronecker product \otimes , applying the coordinate transformation (9) to all states $x_{abc} \in \mathbb{R}^{3n}$ representing three-phase waveforms in the model (1) yields

$$x_{dq0}^{+-}(t) = (I_n \otimes T(t)) \bar{x}_{abc}(t, \tau) \in \mathbb{R}^{6n}, \quad (13)$$

where I_n denotes the $n \times n$ identity matrix. Furthermore, with (10) we have that

$$\begin{aligned} x_{abc}(t) &= (I_n \otimes \mathcal{T}_t(t)) x_{dq0}^{+-}(t), \\ x_{abc}(t - \tau) &= (I_n \otimes \mathcal{T}_\tau(t)) x_{dq0}^{+-}(t). \end{aligned}$$

Hence, from (1) we obtain the following system of differential equations describing the motion of the electrical system in $dq0^{+-}$ -coordinates

$$\begin{aligned} \dot{x}_{dq0}^{+-}(t) &= (I_n \otimes T(t)) \dot{\bar{x}}_{abc}(t, \tau) + (I_n \otimes \mathcal{P}) x_{dq0}^{+-}(t) \\ &:= f^{+-} \left(x_{dq0}^{+-}(t), y_z(t), y_z(t - \tau) \right), \end{aligned}$$

where the function $f^{+-} : \mathbb{R}^{(6n+2q)} \rightarrow \mathbb{R}^{6n}$ describes the motion of the positive, negative and zero sequence components.

The overall system (1) is given in the new coordinates by

$$\begin{aligned} \dot{x}_{dq0}^{+-}(t) &= f^{+-} \left(x_{dq0}^{+-}(t), y_z(t), y_z(t - \tau) \right), \\ \dot{z}(t) &= g(z(t), y_x(t)), \\ y_x(t) &= h^{+-} \left(x_{dq0}^{+-}(t) \right), \quad y_z(t) = w(z(t)), \end{aligned} \quad (14)$$

where $h^{+-} : \mathbb{R}^{(6n+2q)} \rightarrow \mathbb{R}^l$ is the output mapping of the electrical system in $dq0^{+-}$ -coordinates.

The employed coordinate transformation has the following implications:

- To perform a rigorous small-signal analysis, the considered system needs to have an equilibrium point. As shown in Section II-A, given a synchronized solution x_{abc}^* the corresponding dq -components in the positive and negative sequences, i.e., $x_{dq}^{+,*}$, are constant. Hence, by shifting the zero component to the origin via the transformation $\tilde{x}_0^+ = x_0^+ - x_0^{+,*}$ the system (14) has an equilibrium point. Consequently, the employed transformation (9) achieves the fundamental objective of mapping the sinusoidal waveforms $x_{abc}^*(t)$ to an equilibrium point.
- The transformation (9) lifts the $3n$ -dimensional state space of the electrical dynamics in a higher-dimensional space of dimension $6n$. This is done in order to decompose the AC waveforms into their positive, negative and zero sequences. As $T(t)$ is invertible, asymptotic stability of an equilibrium point $(x_{dq0}^{+,*}(t), z^*)$ of the system (14) implies asymptotic convergence of the solutions of the system (1) to the synchronized solution $(x_{abc}^*(t), z^*)$.
- An increase in dimension of the state space also occurs when using the related concept of dynamic phasors to model the system (1) [17]. A main difference between

the here presented approach and the concept of dynamic phasors is that the latter seeks to derive an adequate approximation of the system variables, while the former is an invertible coordinate transformation and, hence, exact.

- The outputs y_z are affected by the time delay τ introduced by the transformation (9). This is a consequence of representing, e.g., three-phase actuation signals such as voltage reference values in $dq0^{+-}$ -coordinates. This aspect is further discussed in the example in Section III, where it is shown that—even if the nonlinear microgrid model contains delays induced by (9)—its small-signal representation may be delay-free. Furthermore, when considering a purely electrical system, i.e.,

$$\dot{x}_{abc}(t) = f(x_{abc}(t)),$$

the transformed system is delay-free, i.e.,

$$\dot{x}_{dq0}^{+-}(t) = f^{+-}(x_{dq0}^{+-}(t)).$$

- In a general unbalanced scenario, the dynamics of the positive and negative sequence variables x_{dq0}^+ , respectively x_{dq0}^- , are coupled and dependent on θ^+ .

III. APPLICATION EXAMPLE

We illustrate the efficacy of the proposed approach by deriving the small-signal model of an exemplary unbalanced microgrid.

A. Nonlinear microgrid model in abc -coordinates

The considered microgrid consists of two inverters connected to a common unbalanced current-controlled load, see Fig. 1. We assume that the inverters are equipped with the standard frequency droop control [5], while their voltage magnitudes are kept constant. The dynamics of the low-level inner current and voltage control loops of the respective inverters are not modeled explicitly, but represented by a first-order low-pass filter. In addition, we assume that these inner control loops are designed such that they provide a balanced terminal voltage even under unbalanced network conditions. This can, e.g., be achieved via PR-controllers, see [25]. Then, the model of the inverter at node i , $i \in \{1, 2\}$, is given by

$$\begin{aligned} \tau_{\delta,i} \dot{\delta}_i &= -\delta_i + \bar{\delta}_i, \\ \dot{\delta}_i &= \omega^d - k_{P,i}(P_i^m - P_i^d), \\ \tau_{m,i} \dot{P}_i^m &= -P_i^m + P_i, \\ v_{abc,i} &= \sqrt{2}V_i \begin{bmatrix} \sin(\delta_i) & \sin(\delta_i - \frac{2\pi}{3}) & \sin(\delta_i + \frac{2\pi}{3}) \end{bmatrix}^\top, \end{aligned} \quad (15)$$

where $v_{abc,i}$ is the three-phase output voltage with phase angle δ_i and RMS amplitude V_i , ω^d is the nominal network frequency, $k_{P,i}$ is the droop gain, P_i^d the active power setpoint, P_i^m the filtered active power, $\tau_{m,i}$ is the time constant of the measurement filter and $\tau_{\delta,i}$ the time constant of the first-order filter used to represent the dynamics of the inner-control loops of the inverter. Furthermore, the active power P_i is given by

$$P_i = v_{abc,i}^\top i_{abc,i},$$

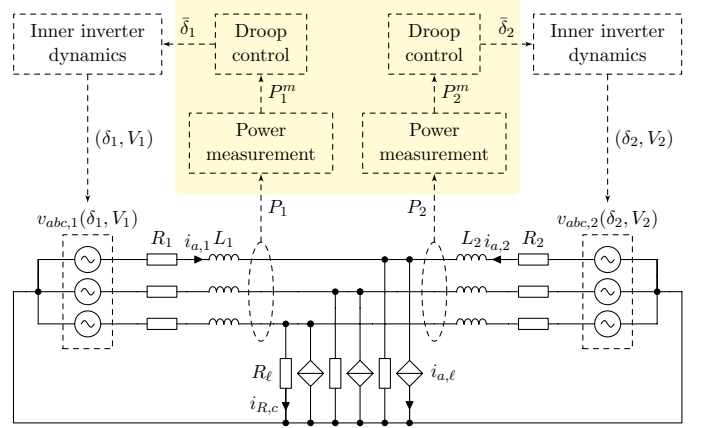


Fig. 1. Microgrid composed of two droop-controlled inverters connected to an unbalanced load. It can be seen that the trajectories obtained with both models match very well.

where $i_{abc,i}$ is the current injected by the inverter.

The unbalanced load is modeled via an unbalanced three-phase current source in parallel to a balanced resistance. From Fig. 1, the voltage across the resistor is given by

$$v_{abc,\ell} = R_\ell i_{abc,R} = R_\ell (i_{abc,1} + i_{abc,2} - i_{abc,\ell}).$$

Furthermore, the power line connecting the i -th inverter to the load at node ℓ is modeled by a balanced RL -element, i.e.,

$$\begin{aligned} L_i \dot{i}_{abc,i} &= -R_i i_{abc,i} + v_{abc,i} - v_{abc,\ell} \\ &= -(R_i + R_\ell) i_{abc,i} + v_{abc,i} - R_\ell i_{abc,k} + R_\ell i_{abc,\ell}, \end{aligned}$$

with $k \in \{1, 2\} \setminus \{i\}$. Hence, with $x_{abc} = (i_{abc,1}, i_{abc,2})$, $z_i = (\bar{\delta}_i, \delta_i, P_i^m)$, $z = (z_1, z_2)$, $y_x = (i_{abc,1}, i_{abc,2})$, $y_z = (v_{abc,1}(\delta_1), v_{abc,2}(\delta_2))$ and $d_x = i_{abc,\ell}$, the overall dynamics can be written compactly in the form of (1), i.e.,

$$\begin{aligned} \dot{x}_{abc} &= (A_x \otimes I_3) x_{abc} + (B_x \otimes I_3) y_z + (D_x \otimes I_3) \begin{bmatrix} I_3 \\ I_3 \end{bmatrix} d_x, \\ \dot{z} &= A_z z + B_z y_z^\top y_x + d_z, \end{aligned} \quad (16)$$

where $B_x = \text{diag}(L_1, L_2)^{-1}$, $D_x = R_\ell B_x$ and $A_z = \text{blkdiag}(A_{z,1}, A_{z,2})$, $b_{z,1} = \begin{bmatrix} \frac{1}{\tau_{m,1}} & 0 \end{bmatrix}$, $b_{z,2} = \begin{bmatrix} 0 & \frac{1}{\tau_{m,2}} \end{bmatrix}$,

$$A_x = \begin{bmatrix} -\frac{R_1 + R_\ell}{L_1} & -\frac{R_\ell}{L_1} \\ -\frac{R_\ell}{L_2} & -\frac{R_2 + R_\ell}{L_2} \end{bmatrix}, A_{z,i} = \begin{bmatrix} -\frac{1}{\tau_{\delta,i}} & \frac{1}{\tau_{\delta,i}} & 0 \\ 0 & 0 & -k_{P,i} \\ 0 & 0 & -\frac{1}{\tau_{m,i}} \end{bmatrix},$$

$$B_{z,i} = \begin{bmatrix} 0_{2 \times 2} & b_{z,1}^\top & 0_{2 \times 2} & b_{z,2}^\top \end{bmatrix}^\top, B_z = \begin{bmatrix} B_{z,1} \\ B_{z,2} \end{bmatrix},$$

$$d_{z,i} = (0, \omega^d + k_{P,i} P_i^d, 0), d_z = (d_{z,1}, d_{z,2})$$

and $\text{blkdiag}(\cdot)$ denotes a block-diagonal matrix.

B. Nonlinear microgrid model in $dq0^{+-}$ -coordinates

Following the procedure outlined in Section II-A, we transform the microgrid model (16) into $dq0^{+-}$ -coordinates. As all

lines are balanced, with \mathcal{P} given in (11), this yields (see (14))

$$\begin{aligned} \dot{x}_{dq0}^{+-} &= (A_x \otimes I_6 + I_2 \otimes \mathcal{P}) x_{dq0}^{+-} \\ &\quad + (B_x \otimes I_6) v_{dq0}^{+-} + (D_x \otimes I_6) \begin{bmatrix} I_6 \\ I_6 \end{bmatrix} T(t) d_x, \end{aligned} \quad (17)$$

$$\dot{z} = A_z z + B_z y_z^\top y_x + d_z,$$

where, see (12), (13),

$$v_{dq0}^{+-} = (v_{dq0,1}^{+-}, v_{dq0,2}^{+-}) = (I_2 \otimes T) \begin{bmatrix} \bar{v}_{abc,1} \\ \bar{v}_{abc,2} \end{bmatrix} \in \mathbb{R}^{12}.$$

By using (10), straightforward calculations give

$$y_z^\top y_x = \left((I_2 \otimes \mathcal{T}_t) v_{dq0}^{+-} \right)^\top \left((I_2 \otimes \mathcal{T}_t) i_{dq0}^{+-} \right) = (P_1, P_2).$$

Note that, since we assume $v_{abc,i}$ are balanced waveforms, $v_{0,i}^+(t) = v_{0,i}^-(t) = 0$ for all $t \geq 0$. Hence, componentwise P_i reads as (see also [25])

$$\begin{aligned} P_i &= P_{0,i} + P_{c,i} \cos(2\theta^+) + P_{s,i} \sin(2\theta^+), \\ P_{0,i} &= v_{d,i}^+ i_{d,i}^+ + v_{q,i}^+ i_{q,i}^+ + v_{d,i}^- i_{d,i}^- + v_{q,i}^- i_{q,i}^-, \\ P_{c,i} &= v_{d,i}^+ i_{d,i}^- + v_{q,i}^+ i_{q,i}^- + v_{d,i}^- i_{d,i}^+ + v_{q,i}^- i_{q,i}^+, \\ P_{s,i} &= v_{d,i}^+ i_{q,i}^- + v_{q,i}^+ i_{d,i}^- - v_{d,i}^- i_{q,i}^+ - v_{q,i}^- i_{d,i}^+. \end{aligned} \quad (18)$$

A comparison of the dynamic behavior of both models (16) and (17) is given in Fig. 2. The models are implemented in Matlab/Simulink. The results show that the trajectories obtained from the original model match very well those obtained with the transformed model, hence validating our chosen coordinate transformation (9).

As outlined in Remark 1, the expression (18) shows that the instantaneous active power contains oscillatory components, see also the related discussions in [13]–[15]. However, compared to SG-based power systems, due to the power measurement filters present in (15) these oscillating components do not have a significant impact on the steady-state frequency in the considered microgrid, see Fig. 2. Therefore, it is admissible to replace the active powers P_i in the model (17) by their corresponding constant components, i.e., $P_{0,i}$. For this case we derive the corresponding small-signal model below.

C. Small-signal model

To compute the linearization of the system (17) around an operating point $(x_{dq0}^{+-,*}, z^*)$, we introduce the error states

$$\Delta x_{dq0}^{+-} = x_{dq0}^{+-} - x_{dq0}^{+-,*}, \quad \Delta z = z - z^*, \quad \Delta \delta = (\Delta \delta_1, \Delta \delta_2).$$

Furthermore, since $v_{abc,i}$ are balanced by assumption, we have that $v_0^{+,*} = 0$ and $v_0^{-,*} = \underline{0}_3$. Consequently, straightforward calculations yield

$$\left. \frac{\partial v_{dq0,i}^{+-}}{\partial \delta_i} \right|_{\delta_i^*} = \sqrt{3} V_i (\cos(\delta_i^* - \theta^+), \sin(\delta_i^* - \theta^+), \underline{0}_4).$$

Hence, by defining

$$\mathcal{U} := \left. \frac{\partial v_{dq0}^{+-}}{\partial \delta} \right|_{\delta^*} \in \mathbb{R}^{12 \times 2},$$

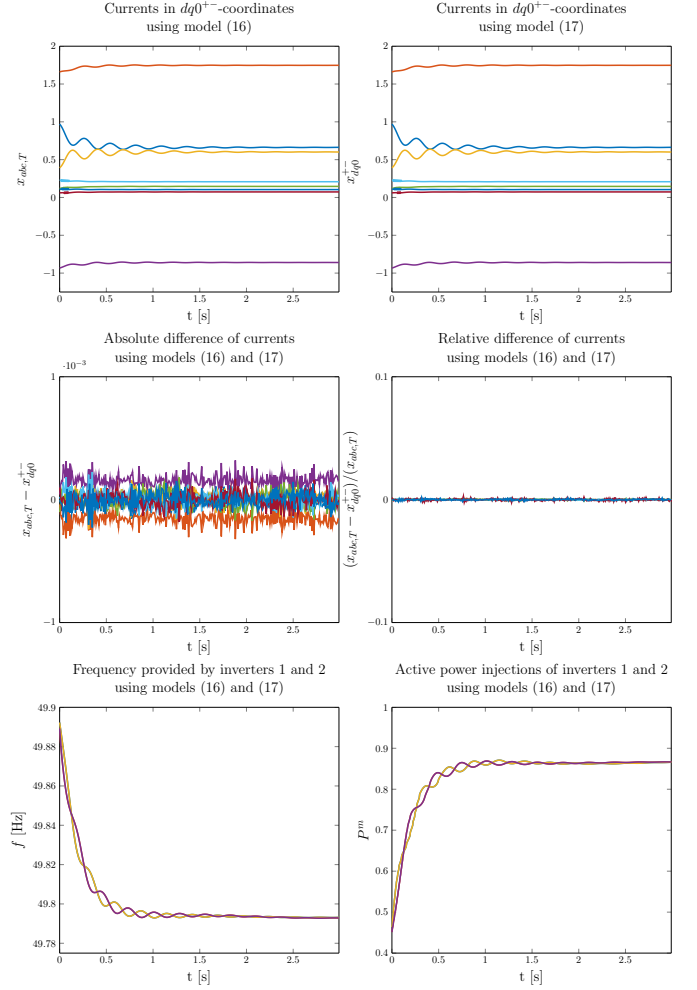


Fig. 2. Comparison of simulation results obtained with the model (16) and the transformed model (17). Unless indicated otherwise, the displayed values are in per unit with respect to $S_{B3\phi} = 3\text{kW}$ and $V_B = 220\text{V}$. Furthermore, $x_{abc,T} = T(t)(x_{abc}(t), x_{abc}(t - \tau))$.

and with $P_i = P_{0,i}$, $i \in \{1, 2\}$, we obtain

$$\begin{aligned} \left. \frac{\partial P}{\partial \delta} \right|_{(\delta^*, x_{dq0}^{+-,*})} &= \mathcal{M} \mathcal{U}, \quad \mathcal{M} = \text{blkdiag}(M_1, M_2) \in \mathbb{R}^{2 \times 12}, \\ \left. \frac{\partial P}{\partial x_{dq0}^{+-}} \right|_{(\delta^*, x_{dq0}^{+-,*})} &= \mathcal{U}^\top \mathcal{N}, \quad \mathcal{N} = \text{blkdiag}(N, N) \in \mathbb{R}^{12 \times 12}, \\ M_i &= \begin{bmatrix} i_{d,i}^{+,*} & i_{q,i}^{+,*} & \underline{0}_4^\top \end{bmatrix}, \quad \bar{N} = \begin{bmatrix} 0 & -1 \\ 1 & 0 \end{bmatrix}, \quad N = \begin{bmatrix} \bar{N} & \underline{0}_{2 \times 4} \\ \underline{0}_{4 \times 2} & \underline{0}_{4 \times 4} \end{bmatrix}. \end{aligned}$$

Thus, the delay-dependent nonlinear dynamics (17) can locally be described by a standard non-delayed linear time-invariant (LTI) system, i.e.,

$$\begin{aligned} \Delta \dot{x}_{dq0}^{+-} &= (A_x \otimes I_6 + I_2 \otimes \mathcal{P}) \Delta x_{dq0}^{+-} + (B_x \otimes I_6) \mathcal{U} \Delta \delta, \\ \Delta \dot{z} &= A_z \Delta z + B_z \left(\mathcal{M} \mathcal{U} \Delta \delta + \mathcal{U}^\top \mathcal{N} \Delta x_{dq0}^{+-} \right). \end{aligned} \quad (19)$$

Furthermore, for the considered setup careful investigation of the right-hand side of (19) shows that locally the dynamics

of the positive, negative and zero sequences are completely decoupled. This is a consequence of the employed coordinate transformation (9) together with the assumptions that $v_{abc,i}$ and the lines are balanced as well as that $P_i = P_{0,i}$, $i = 1, 2$.

With regards to small-signal stability of the system (19), it is straightforward to show that the matrix $(A_x \otimes I_2 + \omega^* I_2 \otimes \bar{N})$ is Hurwitz. Thus, it follows that the negative and zero sequence dynamics represent each a stable LTI system with input zero. Consequently, the operating point $(x_{dq0}^{+,*}, z^*)$, is locally exponentially stable if the origin is an exponentially stable equilibrium point of the linearized positive sequence dynamics given by

$$\begin{aligned} \Delta \dot{x}_{dq}^+ &= (A_x \otimes I_2 + \omega^* I_2 \otimes \bar{N}^\top) \Delta x_{dq}^+ + (B_x \otimes I_2) \Phi \mathcal{U} \Delta \delta, \\ \Delta \dot{z} &= A_z \Delta z + B_z \left(\mathcal{M} \mathcal{U} \Delta \delta + \mathcal{U}^\top \mathcal{N} \Phi^\top \Delta x_{dq}^+ \right), \end{aligned} \quad (20)$$

where $\Phi = \text{blkdiag}([I_2 \quad \mathbf{0}_{2 \times 4}], [I_2 \quad \mathbf{0}_{2 \times 4}])$. The stability analysis for the system (20) can be conducted in the standard small-signal approach, i.e., by investigating the eigenvalues of the system matrix of the positive sequence dynamics (20), as done, e.g., in [7], [8], [11]. Thus, the presented example demonstrates the efficacy of the proposed modeling framework for small-signal analysis of unbalanced microgrids.

IV. CONCLUSIONS AND FUTURE WORK

We have proposed a time-domain modeling framework for small-signal analysis of unbalanced microgrids. At the core of the approach is a suitable coordinate transformation that allows to map a synchronized solution of an unbalanced nonlinear microgrid to an equilibrium point. This is a fundamental prerequisite for any small-signal analysis. The employed coordinate transformation is based on the theory of symmetric components in the time-domain using the "signal delay cancellation" approach. Via the proposed approach, we have derived the small-signal model of an exemplary unbalanced microgrid and shown that—by using the ideas presented in the paper—its small-signal stability can be verified by investigating that of the linearized positive sequence dynamics.

There are several topics to be addressed in future work. The current coordinate transformation provides constant positive and negative sequence components if the synchronized solution of the microgrid possesses a constant frequency. Despite this being a feasible scenario in droop-controlled inverter-based microgrids, we seek to extend the presented ideas to power systems with periodic synchronization frequency. This is relevant when considering networks with synchronous machines. Furthermore, we plan to explore if—by invoking time-scale separation arguments—a similar model reduction as in the balanced scenario (see [21]) can be carried out to obtain a phasor-based representation of the electrical quantities.

REFERENCES

[1] G. Strbac, N. Hatziargyriou, J. P. Lopes, C. Moreira, A. Dimeas, and D. Papadaskalopoulos, "Microgrids: Enhancing the resilience of the European Megagrid," *IEEE Power and Energy Magazine*, vol. 13, no. 3, pp. 35–43, 2015.

[2] N. Hatziargyriou, H. Asano, R. Iravani, and C. Marnay, "Microgrids," *IEEE Power and Energy Magazine*, vol. 5, no. 4, pp. 78–94, 2007.

[3] R. Lasseter, "MicroGrids," in *IEEE PES Winter Meeting*, vol. 1, 2002, pp. 305–308.

[4] F. Katiraei, R. Iravani, N. Hatziargyriou, and A. Dimeas, "Microgrids management," *IEEE Power and Energy Magazine*, vol. 6, no. 3, pp. 54–65, 2008.

[5] J. Guerrero, P. Loh, M. Chandorkar, and T. Lee, "Advanced control architectures for intelligent microgrids – part I: Decentralized and hierarchical control," vol. 60, no. 4, pp. 1254–1262, 2013.

[6] N. L. Sultani, S. A. Papathanasiou, and N. D. Hatziargyriou, "A stability algorithm for the dynamic analysis of inverter dominated unbalanced lv microgrids," *IEEE Transactions on Power Systems*, vol. 22, no. 1, pp. 294–304, 2007.

[7] N. Pogaku, M. Prodanovic, and T. Green, "Modeling, analysis and testing of autonomous operation of an inverter-based microgrid," *IEEE Transactions on Power Electronics*, vol. 22, no. 2, pp. 613–625, Mar. 2007.

[8] G. Diaz, C. Gonzalez-Moran, J. Gomez-Aleixandre, and A. Diez, "Scheduling of droop coefficients for frequency and voltage regulation in isolated microgrids," *IEEE Transactions on Power Systems*, vol. 25, no. 1, pp. 489–496, feb. 2010.

[9] J. W. Simpson-Porco, F. Dörfler, and F. Bullo, "Synchronization and power sharing for droop-controlled inverters in islanded microgrids," *Automatica*, vol. 49, no. 9, pp. 2603–2611, 2013.

[10] J. Schiffer, R. Ortega, A. Astolfi, J. Raisch, and T. Sezi, "Conditions for stability of droop-controlled inverter-based microgrids," *Automatica*, vol. 50, no. 10, pp. 2457–2469, 2014.

[11] J. Schiffer, D. Goldin, J. Raisch, and T. Sezi, "Synchronization of droop-controlled microgrids with distributed rotational and electronic generation," in *52nd IEEE CDC*, Florence, Italy, 2013, pp. 2334–2339.

[12] J. Schlabbach, D. Blume, and T. Stephanblome, *Voltage quality in electrical power systems*. IET, 2001, no. 36.

[13] E. Nasr-Azadani, C. A. Cañizares, D. E. Olivares, and K. Bhattacharya, "Stability analysis of unbalanced distribution systems with synchronous machine and DFIG based distributed generators," *IEEE Transactions on Smart Grid*, vol. 5, no. 5, pp. 2326–2338, 2014.

[14] R. H. Salim, R. A. Ramos, and N. G. Bretas, "Analysis of the small signal dynamic performance of synchronous generators under unbalanced operating conditions," in *PES General Meeting*. IEEE, 2010, pp. 1–6.

[15] R. H. Salim and R. A. Ramos, "A model-based approach for small-signal stability assessment of unbalanced power systems," *IEEE Transactions on Power Systems*, vol. 27, no. 4, pp. 2006–2014, 2012.

[16] Z. Miao, L. Piyasinghe, J. Khazaei, and L. Fan, "Dynamic phasor-based modeling of unbalanced radial distribution systems," *IEEE Transactions on Power Systems*, vol. 30, no. 6, pp. 3102–3109, 2015.

[17] A. M. Stankovic and T. Aydin, "Analysis of asymmetrical faults in power systems using dynamic phasors," *IEEE Transactions on Power Systems*, vol. 15, no. 3, pp. 1062–1068, 2000.

[18] A. M. Stankovic, S. R. Sanders, and T. Aydin, "Dynamic phasors in modeling and analysis of unbalanced polyphase ac machines," *IEEE Transactions on Energy Conversion*, vol. 17, no. 1, pp. 107–113, 2002.

[19] T. H. Demiray, "Simulation of power system dynamics using dynamic phasor models," Ph.D. dissertation, Citeseer, 2008.

[20] P. Kundur, *Power system stability and control*. McGraw-Hill, 1994.

[21] J. Schiffer, D. Zonetti, R. Ortega, A. Stankovic, T. Sezi, and J. Raisch, "A survey on modeling of microgrids—from fundamental physics to phasors and voltage sources," *Automatica*, vol. 74, pp. 135–150, 2016.

[22] S. Sudhoff, "Multiple reference frame analysis of an unsymmetrical induction machine," *IEEE Transactions on Energy Conversion*, vol. 8, no. 3, pp. 425–432, 1993.

[23] Y. Zhou, P. Bauer, J. A. Ferreira, and J. Pierik, "Operation of grid-connected dfig under unbalanced grid voltage condition," *IEEE Transactions on Energy Conversion*, vol. 24, no. 1, pp. 240–246, 2009.

[24] J. He, J. Hu, and X. Wang, "A control strategy for an island operated lv microgrid under unbalanced faults," in *Future Energy Electronics Conference*. IEEE, 2015, pp. 1–6.

[25] R. Teodorescu, M. Liserre et al., *Grid converters for photovoltaic and wind power systems*. John Wiley & Sons, 2011, vol. 29.

[26] J. Rocabert, A. Luna, F. Blaabjerg, and P. Rodriguez, "Control of power converters in AC microgrids," *IEEE Transactions on Power Electronics*, vol. 27, no. 11, pp. 4734–4749, Nov. 2012.